

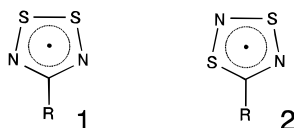
Electronic Excitation of the 1,2,3,5-Dithiadiazolyl Radical. A Spectroscopic and Theoretical Analysis

Jennifer Campbell,^{1a,2} Dieter Klapstein,^{1a,3}
 Peter F. Bernath,^{*,1a} William M. Davis,^{1b}
 Richard T. Oakley,^{*,1b} and John D. Goddard^{*,1b}

The Guelph-Waterloo Centre for Graduate Work in Chemistry, Waterloo Campus, Department of Chemistry University of Waterloo, Waterloo, Ontario N2L 3G1, Canada, and Guelph Campus, Department of Chemistry and Biochemistry, University of Guelph, Guelph, Ontario N1G 2W1, Canada

Received November 29, 1995

The chemistry and molecular and solid state structures of heterocyclic SN- and SeN-containing radicals have been intensively studied in recent years. Derivatives of the isomeric 1,2,3,5- and 1,3,2,4-dithiadiazolyl radicals **1** and **2** have received



particular attention.⁴ In part, this activity can be attributed to the potential use of these materials in the design of molecular conductors.⁵ Of the two isomeric forms, the 1,2,3,5-compounds **1** are the more stable; derivatives of the 1,3,2,4-compounds **2** can be photochemically converted into **1**.⁶ The molecular properties of derivatives of **1** have been studied in solution by ESR spectroscopy⁷ and cyclic voltammetry⁸ and in the gas phase by photoelectron spectroscopy.^{9,10} The results of these studies, in conjunction with those obtained from *ab initio* molecular orbital calculations, have provided a clear picture of the ground

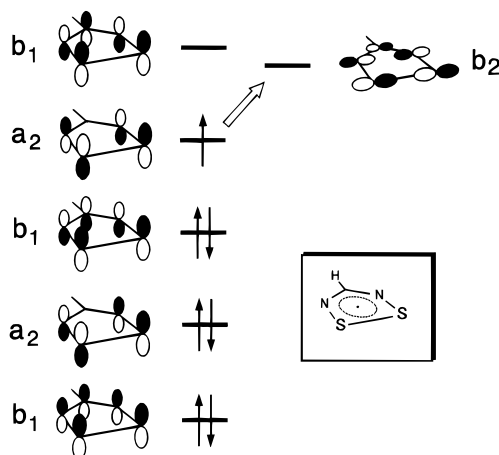


Figure 1. Qualitative MO diagram for [HCN₂S₂], showing the π -orbital manifold and $\pi^* \rightarrow \sigma^*$ excitation.

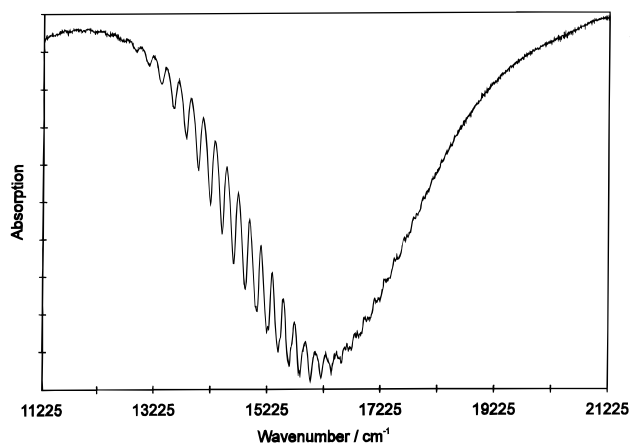


Figure 2. Gas phase electronic spectrum of [HCN₂S₂].

state electronic structure of this class of radical. As illustrated in Figure 1, the singly occupied molecular orbital (SOMO) is an S–S (and S–N) antibonding a_2 orbital. Consistently with this description, which places a node in the distribution of the unpaired electron at the 4-position of the CN₂S₂ ring, the properties of these radicals, e.g., hyperfine coupling constants, solution oxidation and reduction potentials, and gas phase ionization potentials, show little dependence on the nature of the 4-substituent. From a structural perspective, and in accord with the bonding characteristics of the radical SOMO, oxidation of the radical leads to a shortening of the S–S and, to a lesser extent, the S–N bonds. Such changes have been used to diagnose, in a qualitative manner, the degree of charge transfer in the charge transfer salts.¹¹

While these ground state properties are thus well understood, relatively little is known of the excited state electronic structure of **1**. Extensive spectroscopic and theoretical studies on closed-shell electron-rich sulfur–nitrogen heterocycles have established that the rich visible spectra displayed by these compounds originate from $\pi^* \rightarrow \pi^*$ excitations,^{12,13} but the electronic absorp-

- (1) (a) University of Waterloo. (b) University of Guelph.
- (2) Current address: Department of Chemistry, University of British Columbia, 2036 Main Mall, Vancouver, British Columbia V6T 1Y6, Canada.
- (3) Permanent address: Department of Chemistry, St. Francis Xavier University, Antigonish, Nova Scotia B2N 1C0, Canada.
- (4) (a) Cordes, A. W.; Haddon, R. C.; Oakley, R. T. In *The Chemistry of Inorganic Ring Systems*; Stuedel, R., Ed.; Elsevier: Amsterdam, The Netherlands, 1992; p 295. (b) Rawson, J. M.; Banister, A. J. In *The Chemistry of Inorganic Ring Systems*; Stuedel, R., Ed.; Elsevier: Amsterdam, The Netherlands, 1992; p 323. (c) Banister, A. J.; Rawson, J. M.; Lavender, I. *Adv. Heterocycl. Chem.* **1995**, *62*, 137.
- (5) Cordes, A. W.; Haddon, R. C.; Oakley, R. T. *Adv. Mater.* **1994**, *6*, 798.
- (6) (a) Burford, N.; Passmore, J.; Schriver, M. J. *J. Chem. Soc., Chem. Commun.* **1986**, 140. (b) Brooks, W. V. F.; Burford, N.; Passmore, J.; Schriver, M. J.; Sutcliffe, L. H. *J. Chem. Soc., Chem. Commun.* **1987**, 69. (c) Chung, Y.-L.; Fairhurst, S. A.; Gillies, D. G.; Preston, K. F.; Sutcliffe, L. H. *Magn. Reson. Chem.* **1992**, *30*, 666.
- (7) Preston, K. F.; Sutcliffe, L. H. *Magn. Reson. Chem.* **1990**, *28*, 189.
- (8) (a) Boéré, R. T.; Moock, K. H. *J. Am. Chem. Soc.* **1995**, *117*, 4755. (b) Boéré, R. T.; Moock, K. H.; Parvez, M. Z. *Z. Anorg. Allg. Chem.* **1994**, *620*, 1589. (c) Aherne, C. M.; Banister, A. J.; Gorrell, I. B.; Hansford, M. I.; Hauptman, Z. V.; Luke, A. W.; Rawson, J. M. *J. Chem. Soc., Dalton Trans.* **1993**, 967.
- (9) (a) Cordes, A. W.; Goddard, J. D.; Oakley, R. T.; Westwood, N. P. C. *J. Am. Chem. Soc.* **1989**, *111*, 6147. (b) Boéré, R. T.; Oakley, R. T.; Reed, R. W.; Westwood, N. P. C. *J. Am. Chem. Soc.* **1989**, *111*, 1180.
- (10) Cordes, A. W.; Bryan, C. D.; Davis, W. M.; de Laat, R. H.; Glarum, S. H.; Goddard, J. D.; Haddon, R. C.; Hicks, R. G.; Kennepohl, D. K.; Oakley, R. T.; Scott, S. R.; Westwood, N. P. C. *J. Am. Chem. Soc.* **1993**, *115*, 7232.

- (11) (a) Bryan, C. D.; Cordes, A. W.; Fleming, R. M.; George, N. A.; Glarum, S. H.; Haddon, R. C.; MacKinnon, C. D.; Oakley, R. T.; Palstra, T. T. M.; Perel, A. S. *J. Am. Chem. Soc.* **1995**, *117*, 6880. (b) Banister, A. J.; Hansford, M. I.; Hauptman, Z. V.; Luke, A. W.; Wait, S. T.; Clegg, W.; Jørgenson, K. A. *J. Chem. Soc., Dalton Trans.* **1990**, 2793. (c) Bryan, C. D.; Cordes, A. W.; Haddon, R. C.; Hicks, R. G.; Oakley, R. T.; Palstra, T. T. M.; Perel, A. S.; Scott, S. R. *Chem. Mater.* **1994**, *6*, 508.
- (12) (a) Oakley, R. T. *Prog. Inorg. Chem.* **1988**, *36*, 299. (b) Chivers, T. *Chem. Rev.* **1985**, *85*, 341.

Table 1. Calculated Total Energies (au) and S–S and S–N Distances (Å) in the 2A_2 and 2B_2 States of **1** (R = H) at the UHF-Optimized Geometries, in Addition to Excitation Energies Δ (cm^{-1})

basis set	2A_2 ground state			2B_2 excited state			Δ
	energy	$r(\text{S}-\text{S})$	$r(\text{S}-\text{N})$	energy	$r(\text{S}-\text{S})$	$r(\text{S}-\text{N})$	
3-21G*							
UHF	-937.791 05	2.125	1.660	-937.736 11	2.645	1.614	12 058
MP2	-938.308 85			-938.278 55			6 650
MP3	-938.330 01			-938.293 25			8 068
MP4SDQ	-938.349 31			-838.312 31			8 121
6-31G**							
UHF	-942.310 57	2.092	1.652	-942.247 26	2.581	1.617	13 895
MP2	-942.980 70			-942.937 75			9 426
MP3	-943.006 94			-942.958 46			10 640
MP4	-943.053 79			-943.012 87			8 981
6-311G**							
UHF	-942.385 30	2.107	1.648	-942.320 38	2.577	1.614	14 248
MP2	-943.084 55			-943.040 77			9 609
MP3	-943.107 29			-942.057 49			10 930
MP4	-943.160 13			-943.118 27			9 197
6-311+G(2df,p)							
UHF	-942.430 52	2.088	1.631	-942.359 99	2.524	1.601	15 480
MP2	-943.280 22			-943.225 86			11 931

tions responsible for the intense colors exhibited by derivatives of **1** have never been probed in detail. There has been, therefore, a clear need to gain a better insight into the nature of the excited states of these radicals.

Solution measurements of the electronic spectra of dithia-diazolyls are difficult to interpret because of the simultaneous presence (in equilibrium) of the radical and its dimer; both species are strongly absorbing.¹⁴ In order to overcome the problems associated with condensed phase measurements, we have undertaken a combined gas phase spectroscopic and theoretical study of the excited states of the prototypal radical [HCN₂S₂] (**1**, R = H). In a previous paper, we examined, by *ab initio* theory and photoelectron spectroscopy, the ground state electronic structure of this radical and also reported and assigned its gas phase vibrational spectrum.¹⁰ Herein we report the observation and theoretical analysis of its gas phase electronic spectrum. This is the first such characterization of any sulfur–nitrogen heterocycle.

The gas phase spectrum of **1** (R = H) covers a large part of the near-infrared and visible region (Figure 2). It seems to be composed of an underlying “continuum” which peaks near 16 200 cm^{-1} (617 nm) and a long vibrational progression with a spacing of about 250 cm^{-1} near the low-wavenumber edge of the transition. The first member of the vibrational progression cannot be assigned on the basis of our spectrum. The first band that we measure is near 11 938 cm^{-1} , but there is clearly at least one more band to lower wavenumbers. We arbitrarily assume that the band at 11 938 cm^{-1} has $\nu' = 1$. By fitting the first 14 bands from 11 938 to 14 823 cm^{-1} , we obtain the formula

$$T_{\nu-0} = 11678(10) + 250(3)\nu_5 - 1.8(2)\nu_5^2 \text{ cm}^{-1}$$

for the band positions $T_{\nu-0}$, with one standard deviation error in parentheses. This puts the electronic band origin at 11 678 cm^{-1} (or lower) and gives $\nu_5' = 250 \text{ cm}^{-1}$ (or higher).

In order to rationalize the spectrum of this molecule, an extensive computational search was made for any low-lying excited states, at the SCF and CIS levels. This search revealed

only one low-lying excited state involving a b_2 singly-occupied molecular orbital (SOMO) and thus an overall 2B_2 excited state.¹⁵ The total energies and optimized geometries of both the 2A_2 ground and 2B_2 excited states are summarized in Table 1. The calculated excitation energy (Δ) (including zero-point vibrational energy changes) varies somewhat both with basis set and with quantum chemical method, but the values of Δ shown in Table 1 are entirely consistent with the excited 2B_2 state lying *ca.* 11 000 cm^{-1} above the ground state, as observed. Both the ground and excited states are of C_{2v} symmetry at their minimum-energy structures. The major structural change upon excitation is the lengthening of the S–S distance, from 2.09 Å in the ground state (6-311+G(2df,p)) to 2.52 Å in the excited state (6-311+G(2df,p)). This bond lengthening can be rationalized in terms of the SOMOs in the two states. The transition from the ground to the excited state involves the promotion of an electron from the $a_2 \pi^*$ orbital to a $b_2 \sigma^*$ orbital (Figure 1). While both are antibonding with respect to the S–S linkage, the weakening of the S–S bond is expected to be far more pronounced when the upper b_2 orbital is occupied. The total Mulliken overlap population (6-311G**) in the 2A_2 state (0.0900) indicates a small but positive interaction between the two sulfurs. This is decreased to a negative value (–0.0601) in the excited 2B_2 state. These changes are entirely consistent with the observed S–S distances in the two states.

The vibrational fine structure (Figure 2) can be explained by considering that the selection rule for symmetric vibrational modes of a_1 symmetry is $\Delta\nu = 0, \pm 1, \pm 2, \dots$. The observed vibrational interval of *ca.* 250 cm^{-1} can be compared to our computational results, which indicate a low-frequency a_1 vibration in the excited state at 289 cm^{-1} (6-311+G(2df,p)). This low-frequency mode corresponds to an S–S stretching motion. In the ground state, this mode is observed at 475 cm^{-1} ; the calculated frequency is also 475 cm^{-1} (6-311+G(2df,p)). The frequency difference between the ground and excited states reflects again the severe weakening of the S–S bond effected by occupation of the antibonding b_2 orbital.

Experimental and Computational Details

The visible spectrum of **1** (R = H) was recorded on a Bruker IFS120HR Fourier transform spectrometer. The vapor from the solid

- (13) (a) Laidlaw, W. G.; Trsic, M. In *Applied Quantum Chemistry*; Smith, V. H., Ed.; Reidel: Dordrecht, the Netherlands, 1986; p 286. (b) Laidlaw, W. G.; Trsic, M. *Int. J. Quantum. Chem.* **1983**, *17*, 367. (c) Klein, H.-P.; Oakley, R. T.; Michl, J. *Inorg. Chem.* **1986**, *25*, 3194. (14) Passmore, J.; Sun, X. *Inorg. Chem.* **1996**, *35*, 1313.

- (15) The $\tilde{A}^2B_2 - \tilde{X}^2A_2$ electronic transition is allowed with the transition dipole pointing out of the plane in the x direction. Note that our coordinate system has the z direction along the C_2 axis.

dimer¹⁰ was allowed to fill a 1.2 m long White-type multiple-reflector cell. The cell was set for four passes for a total path length of 4.8 m. The spectrometer was operated with a quartz visible beam splitter, a tungsten lamp as a source, and a silicon photodiode detector. Ten thousand scans were recorded at a resolution of 5 cm⁻¹ to obtain, after background corrections, the absorption spectrum shown in Figure 2. The spectrum was corrected with a background scan recorded with an empty cell. The sample integrity was checked by monitoring its vibrational spectrum.

Calculations were performed using Gaussian 92/DFT, revision G.2.¹⁶ In a previous study,¹⁰ we showed that reliable results for the structures and vibrational frequencies of such inorganic ring systems can be

- (16) Frisch, M. J.; Trucks, G. W.; Schlegel, H. B.; Gill, P. M. W.; Johnson, B. G.; Wong, M. W.; Foresman, J. B.; Robb, M. A.; Head-Gordon, M.; Replogle, E. S.; Gomperts, R.; Andres, J. L.; Ragavachari, K.; Binkley, J. S.; Gonzalez, C.; Martin, R. L.; Fox, D. J.; Defrees, D. J.; Baker, J.; Stewart, J. J. P.; Pople, J. A. *Gaussian 92/DFT*, revision G.2; Gaussian Inc.: Pittsburgh, PA, 1993.

obtained using at least a split-valence basis set with added d-type polarization functions. Thus, predictions were made using four sets; 3-21G*, 6-31G** and the larger valence triple- ζ 6-311G** and 6-311+G(2df,p) bases. Geometries and vibrational frequencies were optimized at the UHF level. Energies were determined up to full fourth-order Møller–Plesset (MP4SDTQ).

Acknowledgment. The continuing support of the Natural Sciences and Engineering Research Council of Canada (NSERC) is gratefully acknowledged.

Supporting Information Available: Full listings of optimized geometries and calculated vibrational frequencies of the ground and excited states of **1** (3 pages). Ordering information is given on any current masthead page.

IC951512V